PB83-151753

Experimental Investigations of Fine Particle Charging by Unipolar Ions: A Review

Southern Research Inst.
Birmingham, AL

Prepared for

Industrial Environmental Research Lab.
Research Triangle Park, NC

11 Jul 77

U.S. Department of Commerce
National Technical Information Service
NTIS

TECHNICAL REPORT DATA
(Please read Instructions on the reverse before comp!

1. REPORT NO. EPA-600/J-78-196	2. Journal Article	PB83-151753

4. TITLE AND SUBTITLE: Experimental Investigations of Fine Particle Charging by Unipolar Ions - A Review	5. REPORT DATE: 1978 6. PERFORMING ORGANIZATION CODE
7. AUTHOR(S): *W. B. Smith, L. G. Felix, D. H. Hussey & D. H. Pontius and **L. E. Sparks	8. PERFORMING ORGANIZATION REPORT NO.
9. PERFORMING ORGANIZATION NAME AND ADDRESS: (*) Southern Research Institute, 2000 Ninth St., South Birmingham, Alabama 35205, U.S.A. (**)USEPA, IERL, RTP, NC 27711, U.S.A.	10. PROGRAM ELEMENT NO. 11. CONTRACT/GRANT NO. NA
12. SPONSORING AGENCY NAME AND ADDRESS: EPA, Office of Research and Development, Industrial Environmental Research Laboratory, Research Triangle Park, NC 27711	13. TYPE OF REPORT AND PERIOD COVERED: Journal Article; Apr-Jul '77 14. SPONSORING AGENCY CODE: EPA/600/13

15. SUPPLEMENTARY NOTES

Published in Journal of Aerosol Science, Vol. 9, pp 101-124, 1978 by Pergamon Press, printed in Great Britain.

16. ABSTRACT

The paper gives results of a study relating experimental data to many theories that have been offered in attempts to describe accurately the rate of charge accumulation of fine particles in a unipolar field. The data are reviewed and compiled, and additional particle charging experiments done to extend the quantity of data. Before this study, most experimental data available for comparison with particle charging theories was contained in a 1957 paper by G. Hewitt. Hewitt's experiments were done carefully, but the range of experimental variables was limited and his work was never independently verified. The experiments reported here followed Hewitt's procedures closely and extend the quantity of experimental data. Where there is overlap between this and Hewitt's data, the agreement is good. Experimental results are presented in this paper for the charging rate of particles of 0.109-7 micrometers dia. at various values of electric field strength, ion density and charging time. A limited amount of data is also given which shows the important effects on the charging rate of variations in the particle dielectric constant and the polarity of the corona ion source.

17. KEY WORDS AND DOCUMENT ANALYSIS

a. DESCRIPTORS	b. IDENTIFIERS/OPEN ENDED TERMS	c. COSATI Field/Group
Pollution	Pollution Control	13B
Particles	Stationary Sources	14G
Charging	Unipolar Ions	
Dust		11G
Ions		20H
Polarity		

18. DISTRIBUTION STATEMENT: Release to Public	19. SECURITY CLASS (This Report): Unclassified	21. NO. OF PAGES: 25
	20. SECURITY CLASS (This page): Unclassified	22. PRICE

EPA Form 2220-1 (9-73)

REPRODUCED BY
NATIONAL TECHNICAL
INFORMATION SERVICE
U.S. DEPARTMENT OF COMMERCE
SPRINGFIELD, VA. 22161

EPA-600/J-78-196
JOURNAL ARTICLE

Journal of Aerosol Science, Vol. 9, pp. 101-124 (1978)

EXPERIMENTAL INVESTIGATIONS OF FINE PARTICLE CHARGING BY UNIPOLAR IONS - A REVIEW

W. B. SMITH, L. G. FELIX, D. H. HUSSEY and D. H. PONTIUS
Southern Research Institute, 2000 Ninth Avenue, South Birmingham, Alabama 35205, U.S.A.

and

L. E. SPARKS
Environmental Protection Agency Research, Triangle Park, North Carolina 27711, U.S.A.

(*Received* 4 *April* 1977; *and in revised form* 11 *July* 1977)

Abstract - Many theories have been offered in attempts to describe accurately the rate of charge accumulation of fine particles in a unipolar ion field. There has been little experimental data, however, for comparison with these new theories. In this study, the existing experimental data are reviewed and compiled, and additional particle charging experiments done to extend the quantity of data. Before this study was performed the majority of the experimental data which was available for comparison with particle charging theories was contained in a paper by G. Hewitt, published in 1957. Hewitt's experiments were carefully done, but the range of experimental variables was limited and his work was never independently verified. The experiments reported here followed Hewitt's procedures closely and were designed to extend the quantity of experimental data. There is some overlap between this and Hewitt's data, and in these instances, the agreement is good. Experimental results are presented in this paper for the charging rate of particles of 0.109-7 μm dia. at various values of electric field strength, ion density and charging time. A limited amount of data is also given which shows the important effects on the charging rate of variations in the particle dielectric constant and the polarity of the corona ion source.

NOTATION

E electric field strength
K dielectric constant of the particles
Nt ion density - residence time product
λ molecular mean free path length
μ electrical mobility of the ions

1. INTRODUCTION

1.1 *General discussion*

Many theories have been developed in attempts to describe accurately the charging rate of fine particles by unipolar ions. There has been little experimental data, however, for comparison with these new theories. The objectives of this study were to review and compile the existing experimental data over a wide drange of conditions in order to extend the quantity of data.

Parameters which are known to influence a particle charging rate are the ion density-time product (Nt), the dielectric constant of the particle (K), the electric field strength (E), the particle dia. (d) and the mobility of the charge carriers (μ). Each of these quantities was a variable during the experiments reported here.

Since the primary purpose of this paper is to bring together a body of experimental data, the procedures used to obtain the new data, which followed closely those of Hewitt (1957), are only summarized. A detailed description of all the experimental devices and procedures is available elsewhere (Pontius *et al.*, 1977).

The following paragraphs summarize the results of experiments performed by earlier workers. Section 2 is a short description of our experimental procedures and Section 3 contains the results of our experiments.

1.2 *Review of published results from experimental charging experiments*

1.2.1 *Fuchs et al. (1936).* In their experiments, the authors measured the charging rate of oil mist droplets approximately 1–6 μm in dia. and compared the results with the field charging equation of Rohmann (1923) and Pauthenier and Moreau-Hanot (1932). The mist was formed by condensation, passed through a wire cylinder corona charging device and the charge measured by the "photographic oscillation method". In this method, the droplets were allowed to fall under the influence of gravity and simultaneously were forced by an alternating electric field to oscillate in a horizontal direction. Using photographs of the zig-zag paths of the droplets, the size is first determined from the rate of fall, and then charge is found from the horizontal velocity. For comparison with theory, a value of 1.75×10^{-4} m^2/V sec was assumed as the ion mobility. Figures 1, 2 and 3 contain the experimental data of Fuchs *et al.* The solid line is the value of charge predicted by the classical field charging equation. Experimental problems limited the data to low values of electric field and ion density and consequently the limit or saturation charge was not attained.

1.2.2 *Pauthenier and Moreau-Hanot* (1932). In this theoretical and experimental study the law of particle charging, now referred to as the "classical field charging equation", was derived and verified for large particles.

In order to measure the saturation charge for spherical particles moving through an electric field, two procedures were used. First, to measure the limit charge for large particles, conducting and insulating spheres with dia. of the order of 1 mm–1 cm were dropped

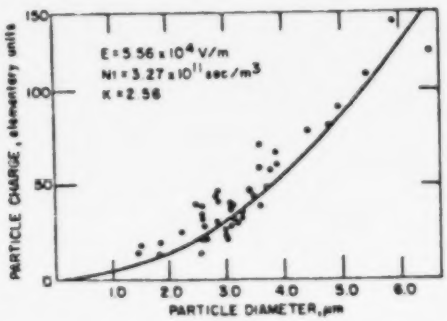

Fig. 1. Charge per particle for a mineral oil aerosol charged in a negative ion field. $Nt = 3.27 \times 10^{11}$ sec/m^3. After Fuchs *et al.* (1936).

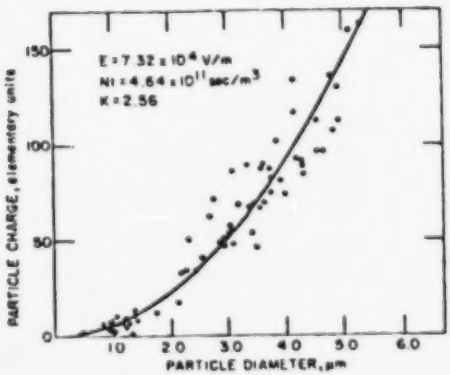

Fig. 2. Charge per particle for a mineral oil aerosol charged in a negative ion field. $Nt = 4.64 \times 10^{11}$ sec/m^3. After Fuchs *et al.* (1936).

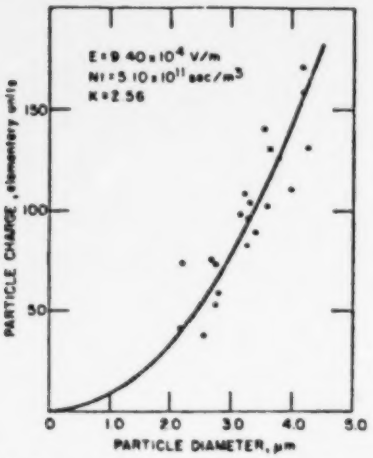

Fig. 3. Charge per particle for a mineral oil aerosol charged by negative ions. $Nt = 5.10 \times 10^{11}$ sec/m^3. After Fuchs *et al.* (1936).

from rest through a wire-cylinder corona device. Their acquired charge was measured by discharge through an electrometer. The theory was verified to within an experimental uncertainty of 1–2%. Second, small conducting and insulating spheres with dia. of the order of 20–200 μm were dropped from rest in the field and their trajectories were photographed. The pictures were analyzed for evidence of deviation from a theoretically determined trajectory based on the effects of gravity and field charging rate, corrected for viscous forces and initial charge. Once again, the experimental results and theoretical predictions were in good agreement. This second technique is called the "method of trajectories". Particles were also collected on the side of the cylinder on wet gelatin plates. This procedure allowed accurate measurements of the number of particles of a particular size which move through a precisely determined vertical distance.

The authors clearly demonstrate the validity of the field charging equations for particles larger than 10 μm dia. In particular, an interesting result is the dependence of the saturation charge upon the particle dielectric constant, which was predicted by the theory and proven experimentally.

1.2.3 *Arendt and Kallman (1926).* These authors used a modified Millikan oil drop apparatus to test their newly developed ion-diffusion charging equation. This equation predicts that a particle charging rate (for any instantaneous net charge) will be proportional to the particle surface area and the ion space charge density. For a long charging time, the rate decreases to a very low value. The charge at this condition was referred to as the limit charge. Table 1 shows the limit charge measured by Arendt and Kallman for several combinations of charging condition and particle dia.

1.2.4 *White (1951).* In this review of particle charging, White discusses theories and experiments related to the electrical precipitation process. A more general derivation of the

Table 1. Experimental charging data of Arendt and Kallman

Particle dia., μm	No. of ions/cm^3	t, (sec)	Q, elementary charge units
1.0	515	1,500	20
1.0	515	3,000	32
1.0	515	6,000	40
4.5	67,000	1,500	170
4.5	67,000	3,000	260
4.5	67,000	6,000	280

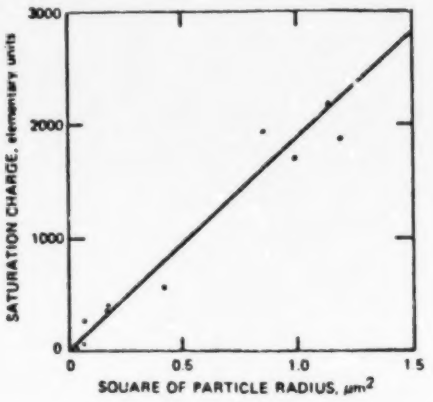

Fig. 4. Experimental results showing linear relation between particle charge and square of particle radius. After White (1951).

diffusional charging equation than that of Arendt and Kallman is presented and some previously unpublished experimental results are given.

The experimental results were obtained by passing an oil mist through a tube-type precipitator. The charge and diameter of individual particles were measured by the Millikan oil-drop method. Figure 4 shows results from an experiment where the charging time was 0.5 sec, and the average field was 5.6 kV/cm. The straight line shown in Fig. 4 is the saturation charge calculated from the field charging equation with the magnitude of the electric field set equal to 1.5 times the average field in the precipitator.

1.2.5 *Penney and Lynch (1957).* The authors report experimental results for particle charge vs the particle dia., the charging electric field strength and the charging time. The monodisperse test aerosols were generated from dioctyl phthalate (DOP) by condensation. and ranged in dia. from 0.3 to 0.64 μm. The magnitude of the charging field was varied from 1.2 to 3.8 kV/cm. Two methods of charging were used, a wire-cylinder device and a rectangular charger. In the latter device the charging zone was bounded by parallel screens through which ions could penetrate and wherein the electric field, charging time and ion density were precisely known. The mean particle charge for various charging conditions was measured either by means of a parallel-plate mobility analyzer or by determination of weight and electrical current associated with collection of charged particles on a filter.

The results and observations of Penney and Lynch were as follows:

The experimentally measured particle charges were higher than the diffusional charging theory predicted if the charging field exceeded about 4000 V/cm.

At extremely high electric field strengths, on the order of 13,000 V/cm, negative corona charging yielded results approximately 50% higher than positive corona. This discrepancy was attributed to the presence of unattached electrons which have an electric mobility much higher than gaseous ions.

The experimental results are shown in Figs 5–8.

1.2.6 *Hewitt (1957).* The classic particle charging experiments of Hewitt have represented the primary source of experimental data on particle charging for 20 years. Experimental results are reported on the charging of particles in air vs particle dia., electric field strength. ion concentration and charging time. These data include particle dia. ranging from 0.14 to 1.32 μm and electric field strengths of 300–10,000 V/cm.

Monodisperse DOP aerosols were produced by means of a condensation aerosol generator and passed through a charging device, a modified wire-pipe corona system. A segment of the pipe electrode, made of wire screening, served to allow ions to pass from the corona zone into the charging zone outside the cylindrical body of the device. The charging time, t, the ion density, N and the electric field, E were closely monitored. In all of his experiments, Hewitt used the value 1.6 cm^2/V sec for ion mobility.

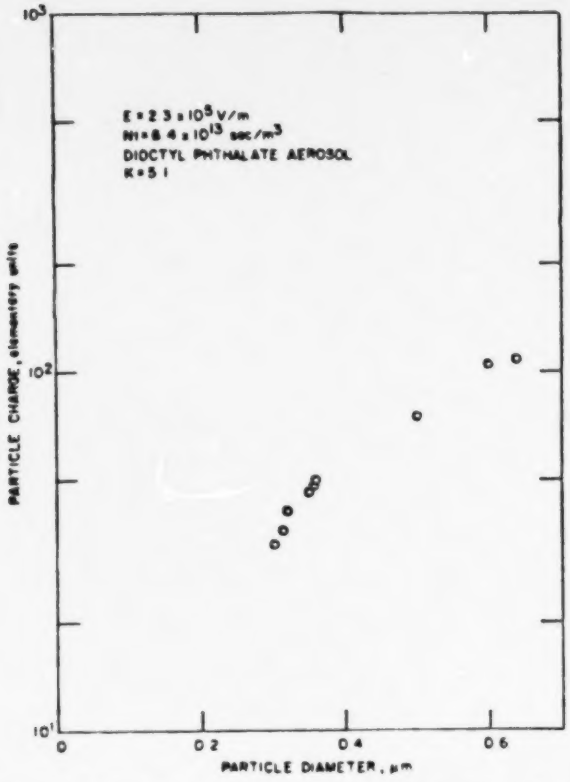

Fig. 5. Particle charge as a function of particle dia. for a dioctyl phthalate aerosol. After Penney and Lynch (1957).

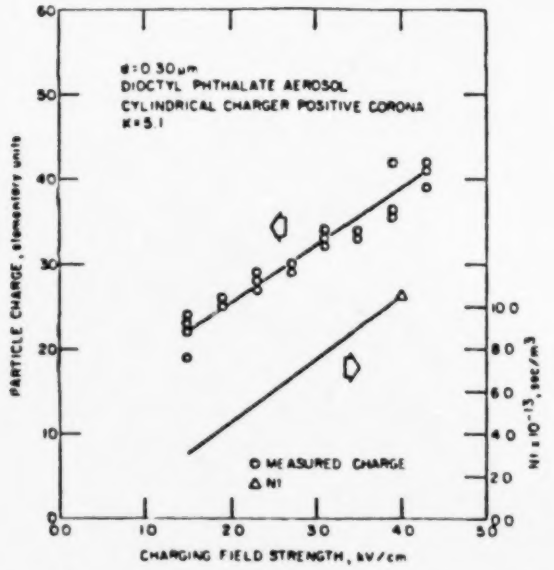

Fig. 6. Particle charge vs the charging field strength for 0.30 μm dia. dioctyl phthalate particles in a positive corona. After Penney and Lynch (1957).

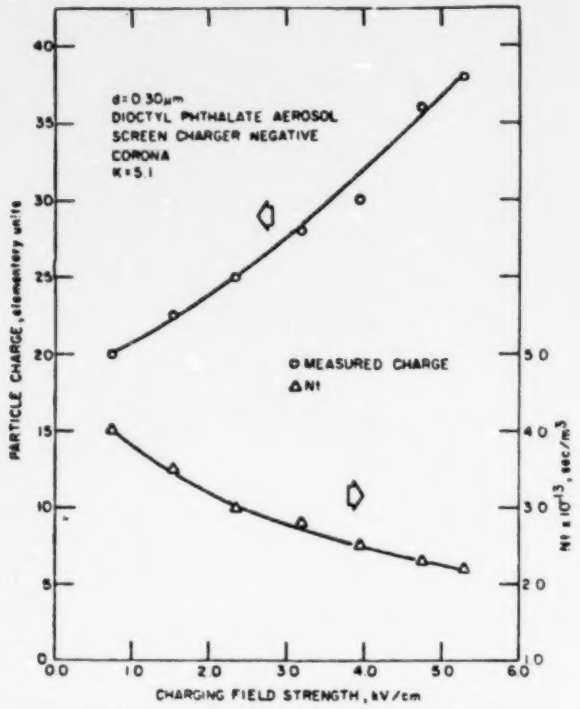

Fig. 7. Particle charge vs the charging field strength and ion density-time product for a 0.30 μm dia. dioctyl phthalate aerosol in a negative ion field. After Penney and Lynch (1957).

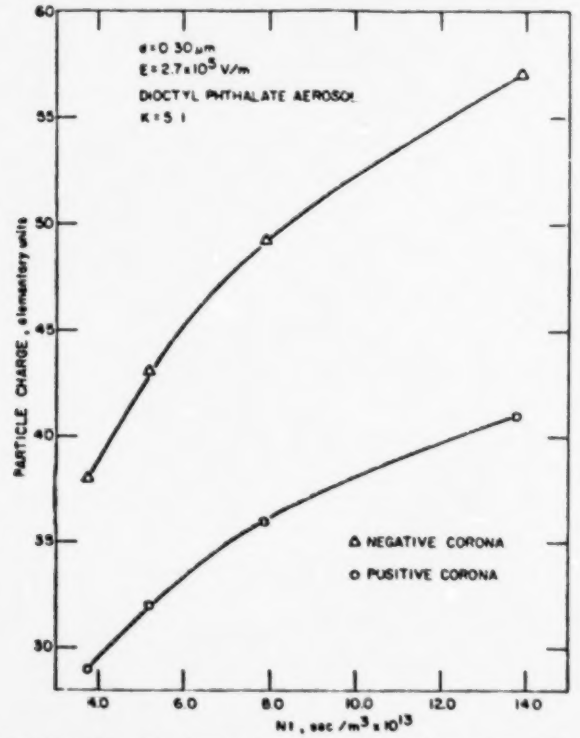

Fig. 8. Comparison of particle charging for negative and positive corona acting on 0.30 μm dia. dioctyl phthalate particles. After Penney and Lynch (1957).

The particle mobility was measured directly using a mobility analyzer, which determined the particle trajectory between a pair of concentric cylinders with laminar, axial air flow and a radial electric field.

Hewitt's experimental results are shown in Figs 9–16 and may be summarized as follows:

For each charging condition there is a particle dia. for which the electrical mobility is a minimum.

The additional charge produced by a charging field is approximately proportional to the magnitude of the field.

The applied field had a significant effect on particle charging for all particle sizes tested.

The measured particle charge depends on the product Nt and not on either N or t independently.

In the absence of an external field, the diffusional charging theory agrees reasonably well with experiment.

For large particles and high electric field strengths (dia. $\geq 1.0\,\mu$m, $E > 3$ kV/cm) the field charging equation of Pauthenier and Moreau-Hanot agrees well with experiment.

1.2.7 *Cochet (1961)*. An aerosol made of shellac was entrained in an electric field and exposed to positive ions for varying periods of time. After charging, the particles were passed through a parallel plate capacitor where a uniform electric field was applied. The capacitor thus acted as a precipitator for these particles. An experimental study was made using an electron microscope to examine the relationship between particle dia. and the position where precipitation on the capacitor/precipitator plate occurred.

As Pauthenier had observed earlier the size spectrum of the precipitated particles was not single valued. Figure 17 is a graph of the calculated electrical mobility vs particle

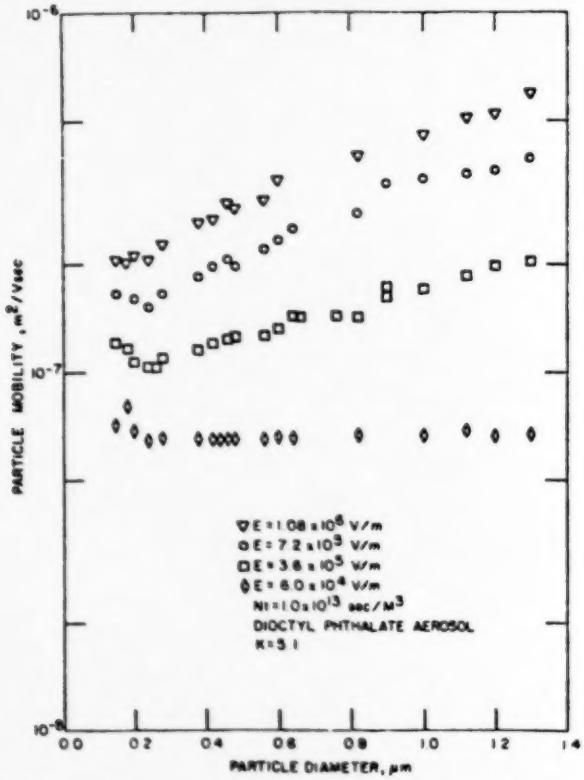
PARTICLE MOBILITY, m²/Vsec
PARTICLE DIAMETER, μm
▽E = 1.08 x 10⁶ V/m
○E = 7.2 x 10⁵ V/m
□E = 3.8 x 10⁵ V/m
◇E = 8.0 x 10⁴ V/m
Nt = 1.0 x 10¹³ sec/m³
DIOCTYL PHTHALATE AEROSOL
K = 5.1

Fig. 9. Electrical mobility of dioctyl phthalate droplets as a function of particle dia. Positive corona charging. After Hewitt (1957).

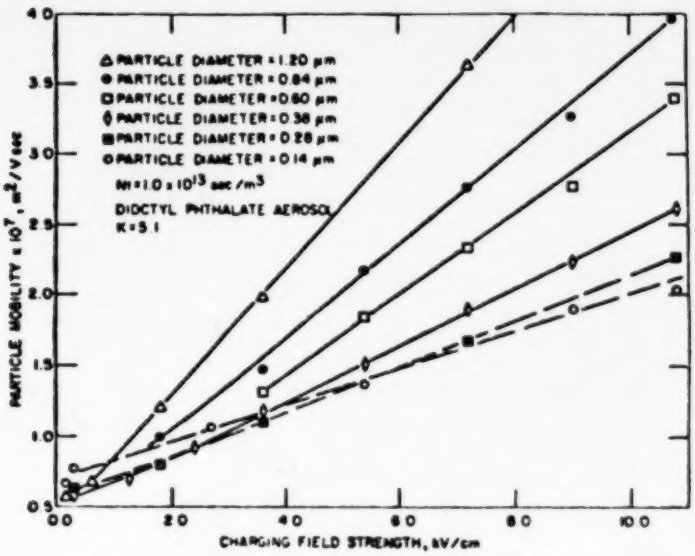
PARTICLE DIAMETER = 1.20 μm
PARTICLE DIAMETER = 0.84 μm
PARTICLE DIAMETER = 0.60 μm
PARTICLE DIAMETER = 0.38 μm
PARTICLE DIAMETER = 0.28 μm
PARTICLE DIAMETER = 0.14 μm
Nt = 1.0 x 10^13 sec/m^3
DIOCTYL PHTHALATE AEROSOL
K = 5.1
PARTICLE MOBILITY x 10^7, m^2/V sec
CHARGING FIELD STRENGTH, kV/cm

Fig. 10. Particle mobility vs the charging field strength for a dioctyl phthalate aerosol under positive corona charging. After Hewitt (1957).

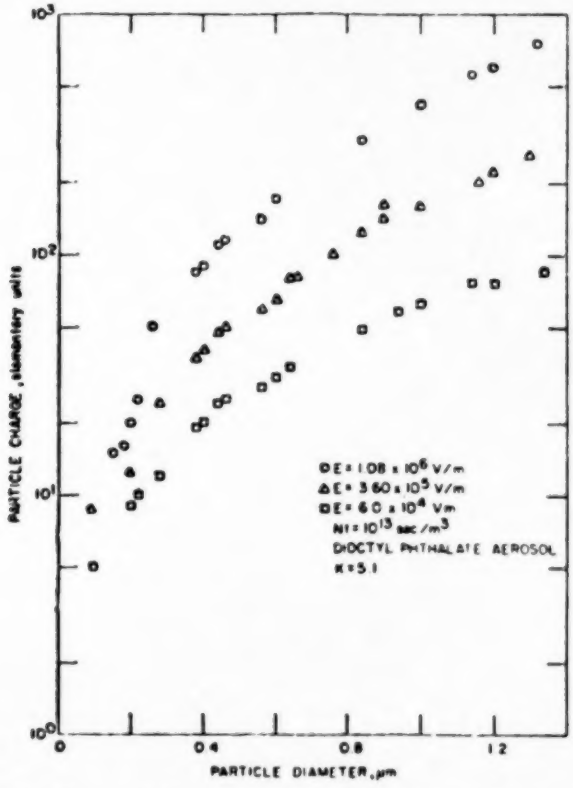
E = 1.08 x 10^6 V/m
E = 3.60 x 10^5 V/m
E = 6.0 x 10^4 V/m
Nt = 10^13 sec/m^3
DIOCTYL PHTHALATE AEROSOL
K = 5.1
PARTICLE CHARGE, elementary units
PARTICLE DIAMETER, μm

Fig. 11. Charge per particle vs particle dia. for a dioctyl phthalate aerosol under positive corona charging. After Hewitt (1957).

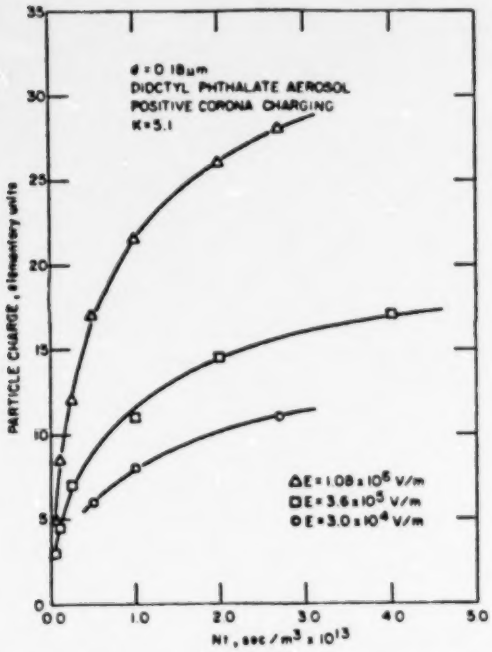

Fig. 12. Charge per particle vs the ion density-residence time product, Nt in a positive corona for 0.18 μm dia. dioctyl phthalate particles. After Hewitt (1957).

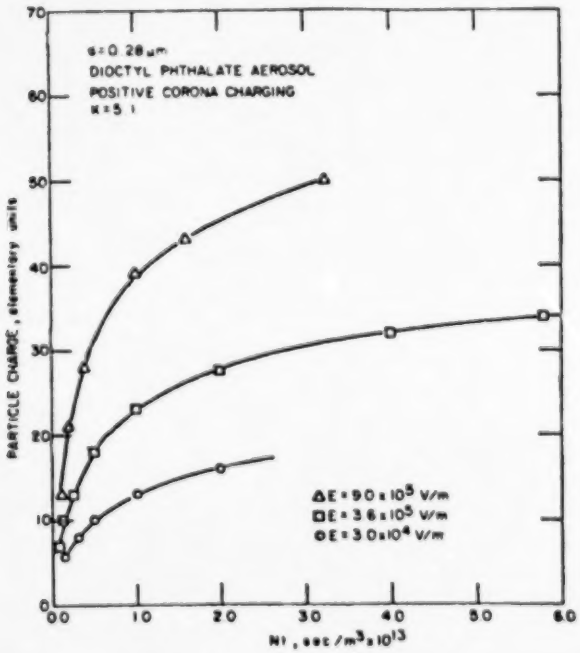

Fig. 13. Charge per particle vs the ion density-residence time product, Nt in a positive corona for 0.28 μm dia. dioctyl phthalate particles. After Hewitt (1957).

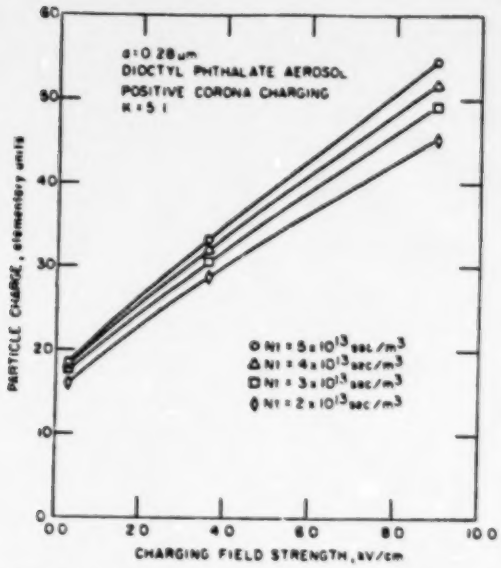
a = 0.28 μm
DIOCTYL PHTHALATE AEROSOL
POSITIVE CORONA CHARGING
K = 5.1
PARTICLE CHARGE, elementary units
CHARGING FIELD STRENGTH, kV/cm
○ N1 = 5 x 10^13 sec/m^3
△ N1 = 4 x 10^13 sec/m^3
□ N1 = 3 x 10^13 sec/m^3
◊ N1 = 2 x 10^13 sec/m^3

Fig. 14. Particle charge vs the charging field strength for 0.28 μm dia. dioctyl phthalate particles. After Hewitt (1957).

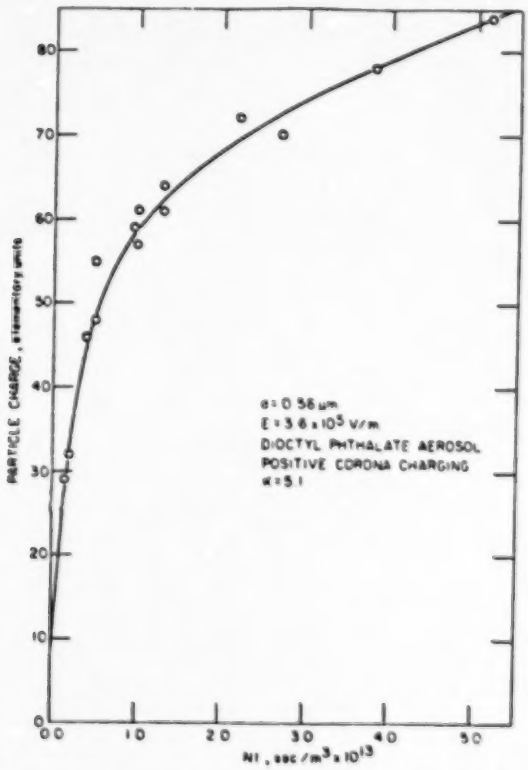

Fig. 15. Particle charge vs the ion density-residence time product for 0.56 μm dia. dioctyl phthalate particles. After Hewitt (1957).

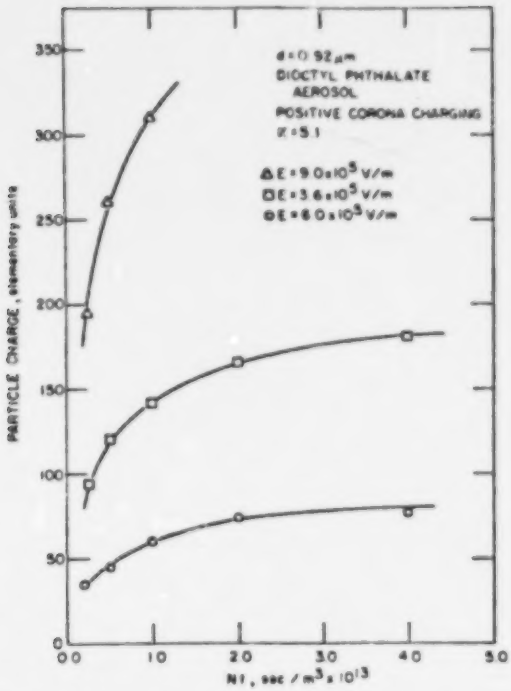

Fig. 16. Particle charge vs the ion density-residence time product for 0.92 μm dia. dioctyl phthalate aerosol particles. After Hewitt (1957).

dia. for two charging conditions. The graph shows a minimum near 0.2 μm particle dia.

1.2.8 *Liu et al. (1967).* Experiments were performed by these authors to study the diffusion charging process at various pressures in order to obtain data for comparison with the existing theories. Monodisperse aerosols were generated by the atomization–condensation method as in the experiments of Hewitt, and Penney and Lynch. The aerosol charging device was also similar to those of Hewitt, and Penney and Lynch; but in addition was equipped to measure the ion mobility by the time-of-flight method. The mobility analyzer was a concentric cylindrical device, similar to Hewitt's. As the voltage between the center rod and the outer cylinder was varied, changes in the current carried by the fraction of the aerosol which penetrated the mobility analyzer were detected by means of an electrometer.

Liu *et al.* measured the ion mobility to be 1.1 cm^2/V sec at a pressure of one atmosphere and determined that the mobility varied inversely as pressure.

Figure 18 shows the experimental results obtained by these authors. These curves were obtained using the value for ion mobility mentioned above and other parameters as shown in the figure legend.

2. EXPERIMENTAL PROCEDURES

The experimental procedures used for the study described in this paper were selected for maximum accuracy and flexibility in investigating the particle charging process over a wide range of conditions, especially those of importance in electrostatic precipitation. The particle charger and mobility analyzer were similar to those reported by Hewitt (1957). The aerosol generators used were a vibrating orifice type and a Collison type. The particle detectors were a Royco Model 225 optical particle counter and an Environment One, Model Rich 100 condensation nuclei counter. The application of each of these devices to the investigation of particle charging is described briefly below.

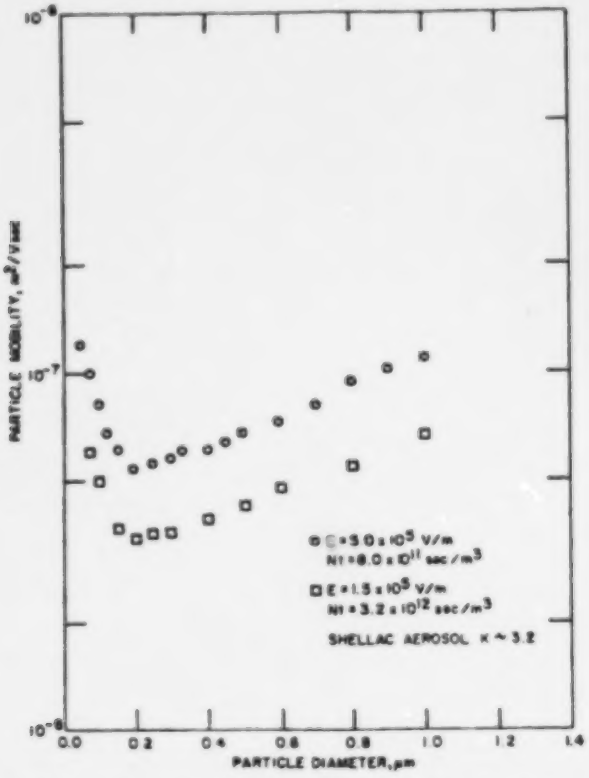

Fig. 17. Particle mobility vs dia. for shellac aerosol particles charged in a positive ion field. After Cochet (1961).

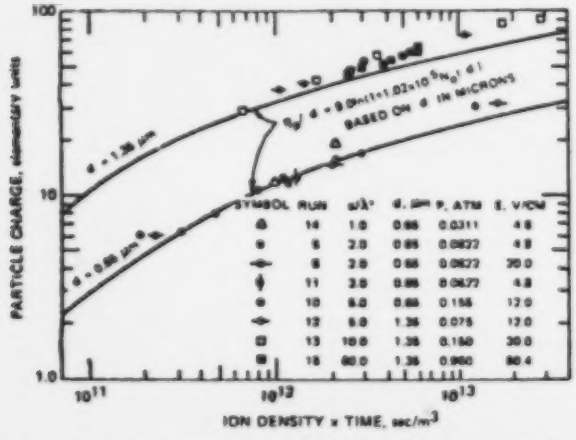

Fig. 18. Experimental charge on aerosol. $\lambda = 0.01\ \mu m$ at $P = 1.0$ ATM. After Liu *et al.* (1967).

2.1 *Aerosol generators*

Two types of aerosol generators were used to cover the range of interest in particle size and dielectric constant. A vibrating orifice aerosol generator (VOAG) was used to create monodisperse DOP aerosols from 1.0 to 7.0 μm dia. The dielectric constant for DOP is 5.1. A detailed description of this type of aerosol generator and its use has been given by Berglund and Liu (1973).

A Collison nebulizer was used to disperse monodisperse plastic spheres from suspensions. Although such a technique necessarily results in a background aerosol created from nonvolatile residues in the suspension liquid, this secondary aerosol is polydisperse and continuous. Therefore it was possible in all of the tests to resolve the sharp peak in measured mobility corresponding to the primary monodisperse aerosol. The dielectric constant of these spheres is approximately 2.2 for polyvinyltoluene (PVTL) and 2.5 for polystyrene latex (PSL). The particle sizes used ranged from 0.109 to 2.02 μm dia.

2.2 *Particle charger*

Figure 19 shows the Hewitt type charger that was used for these experiments. The test aerosol was passed between the grounded screen grid and a metal plate. A high voltage square wave was applied between the screen and plate to establish an electric field for charging. The square waveform was necessary to minimize precipitation of the test aerosol. A d.c. voltage of the same amplitude as the square wave was applied and the current was measured in order to calculate the ion density N from the relationship: $N = j/e\mu E$, where E is the electric field strength in the charging region, j is the current density, μ is the ion mobility and e is the elementary unit of charge.

The calculated field strength was taken to be the value on the surface midway between the two cylindrical boundaries of the charging region, using a zero space charge approximation. Current continuity was then used as the basis for determining the current density and hence the ion density. Comparison with the average value of the field computed with the inclusion of space charge at ten equally spaced points across the charging region indicates that in the worst case the error in the value used for the field was less than 5%.

The charging time was determined from the aerosol flow rate and the geometry of the system. The I–V characteristic of the wire-cylinder corona system was used to derive the ion mobility by means of the procedure described in Section 3.

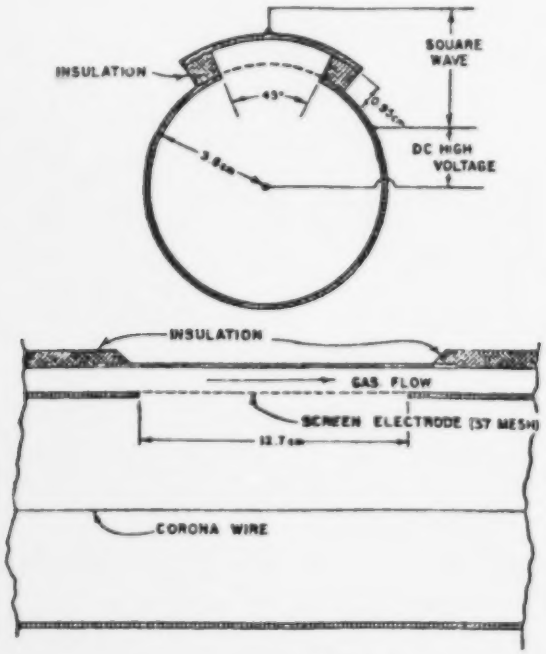

Fig. 19. Cylindrical geometry "Hewitt-type" particle charger. Ions originating at the corona wire pass through the screen electrode into the charging region between the screen and the center plate electrode.

2.3 *Particle mobility analyzer*

Measurements of electrical mobility of charged particles were made by determining particle trajectories in an electric field. Figure 20 is a drawing of the mobility analyzer, based on a concentric cylinder geometry and similar to that used by Hewitt in performing his experiments. Filtered air flows the length of the mobility analyzer under laminar flow conditions. Charged particles enter through a narrow annular passage and experience a radial force toward the central cylinder due to the applied field between the inner and outer cylinders. By moving the scanning slit axially to find the end point of the particle trajectory, the mobility of the charged particles can be determined. Since the particle mobility bears a well defined relationship to the charge, a measurement of the mobility is sufficient to determine the charge. The overall dimensions of the instrument are dictated by the resolution that is desired and the requirement that laminar flow be maintained between the concentric cylinders.

The scanning slit was driven through a system of gears by a reversible electric motor. The position of the slit was determined by the voltage on a potentiometer and displayed as the abscissa on an x–y recorder. A typical scan is shown in Fig. 21 where the ordinate is the analog response of the Royco particle counter. The voltage between the concentric cylinders was adjusted so that the peak in the detector output appeared near the center of the scan. The peak of the mobility distribution could usually be measured with a resolution of ± 1 cm, resulting in an uncertainty of 3–10% in the particle mobility. The peak of the distribution was taken to represent the mean particle mobility.

2.4 *Particle detectors*

A 500 μCi polonium-210 alpha particle source was placed in the outlet of the mobility analyzer to discharge the particles and thus to prevent ambiguous results due to interaction of the particle charge and the sample lines and detectors. A sample was taken through the slit continuously at a flow-rate of 0.1 ft^3/min. This sample was passed to the Royco counter for particles having diameters greater than 0.3 μm, or for smaller particles, to the Environment One condensation nuclei counter. The analog signals from the detectors were displayed on the ordinate of the x–y recorder. Since only the relative concentration over single runs was of interest, calibration and accuracy of the detectors were not critical.

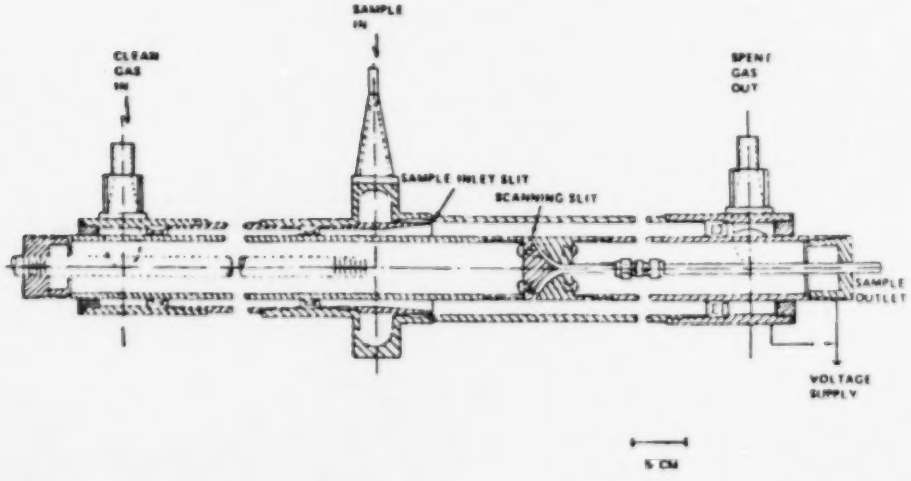

Fig. 20. Mobility analyzer for measuring fine particle charge.

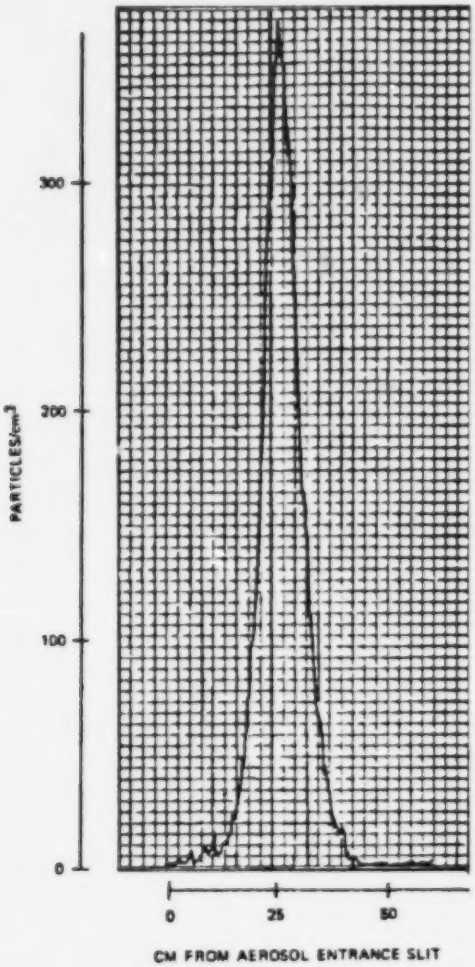

Fig. 21. Strip chart record of a scan made with the Mobility Analyzer. 1.0 μm DOP aerosol.

3. RESULTS

The parameters thought to be most important in charging fine particles are the magnitude of the electric field, the particle size, the ion density-time product, the particle dielectric constant and the ion mobility. Attempts were made during this study to investigate each of these and the results are reported in this section.

3.1 *Ion mobility measurements*

The aerosols used in the charging experiments were derived by evaporation of the liquid from solutions or suspensions containing the desired aerosol material. Molecules from the liquid are thus present in the charger and will affect the ion mobility. The liquids most frequently used were water and methanol.

In order to determine the ion mobility, I–V characteristics of the charger were measured with a vapor present in the concentration normally resulting from aerosol generation. A non-linear curve fit was then applied, using the following theoretical expression relating the current (I) and voltage (V) in a cylindrical corona system (Oglesby and Nichols, 1970):

$$V = \frac{V_0}{\ln b/a}\left\{\left(\ln\frac{b}{a}\right) - 1 + \sqrt{1 + \frac{b^2 I}{2\pi\varepsilon_0\mu L}\left(\frac{\ln b/a}{V_0}\right)^2} - \ln\left[\tfrac{1}{2} + \tfrac{1}{2}\sqrt{1 + \frac{b^2 I}{2\pi\varepsilon_0\mu L}\left(\frac{\ln b/a}{V_0}\right)^2}\right]\right\}.$$

where b = cylinder radius, a = corona wire radius, L = length of corona wire, V_0 = corona inception voltage, μ = ion mobility and ε_0 = permittivity of air.

The measured I–V characteristics of the charger are presented in Fig. 22 for air saturated with vapors of water and methanol. Curve fitting was done to the lower part of each of the curves (current less than 2 mA) where anomalous behavior, such as inhomogeneous current, thermal effects, etc. are least likely to occur. The resulting mobility values for positive corona were 2.38 cm^2/V sec for H_2O in air and 2.03 cm^2/V sec for methanol. A value of 2.70 cm^2/V sec was determined for negative corona and an H_2O suspension liquid. Differences in the I–V characteristics for ion mobilities of 2.03 and 2.38 cm^2/V sec are easily resolved. A change of about half that amount will represent an approximate limit of sensitivity, about 8%.

Bricard (1972) has reported results of mobility measurements which indicate effects of ion aging. When the ion lifetime is increased, by decreasing the applied voltage or increasing the electrode separation, the measured mobility decreases. Apparently the more mobile ion species are quickly depleted from the conducting medium. For ion lifetimes less than 1 msec, as in our charging device, Bricard reports a mobility of 2.3 cm^2/V sec for positive corona in dry air, which is within 5% of our determination for air saturated with water vapor. The average ion mobility for negative corona is thought to be higher because of the contribution of free electrons in the corona current.

3.2 *Particle charge vs electric field strength*

Extensive tests to determine the relationship between particle charge and electric field strength were performed using PVTL, PSL and DOP particles. Also, a range of particle sizes was tested.

According to theory, the saturation charge due to field charging should be directly proportional to the field strength with some dependence on the dielectric constant. Since field charging is the dominant mechanism for large particles (dia. > 1 μm) and moderate fields, one would expect the observed charge to vary directly with the field strength. Figure 23 contains data for 1 and 2 μm dia. DOP particles which demonstrate this phenomenon. The deviation from a linear dependence at very high fields is attributed to turbulence introduced by the corona wind and to an increase in ion mobility as observed by Bricard. The data

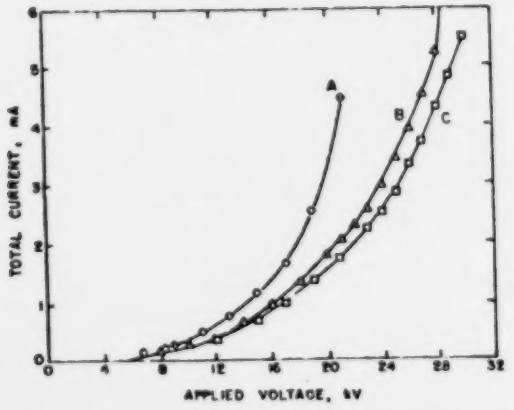

Fig. 22. Charger I–V characteristics for three gaseous media. (A) Water vapor in air and negative corona. (B) Water vapor in air, positive corona. (C) Methanol in air, positive corona.

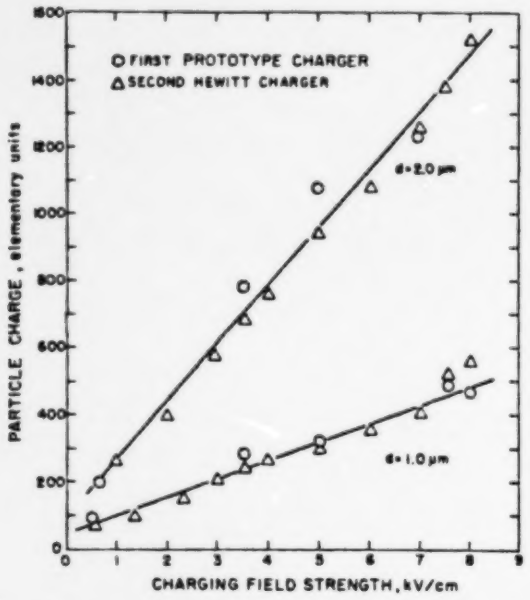

Fig. 23. Comparison of particle charging vs charging field strength for two different Hewitt-type chargers. The Nt product was held constant at 1.0×10^{13} sec/m^3, and the field was varied. Aerosols used were DOP, 1.0 and 2.0 μm in dia.

reported in this paper were all taken at electric field values low enough to avoid confusion due to these effects. Additional data for various DOP particle sizes and electric field strength are contained in the remaining figures, plotted in a different way.

Figures 24, 25 and 26 contain data showing similar data for PSL spheres. The dependence

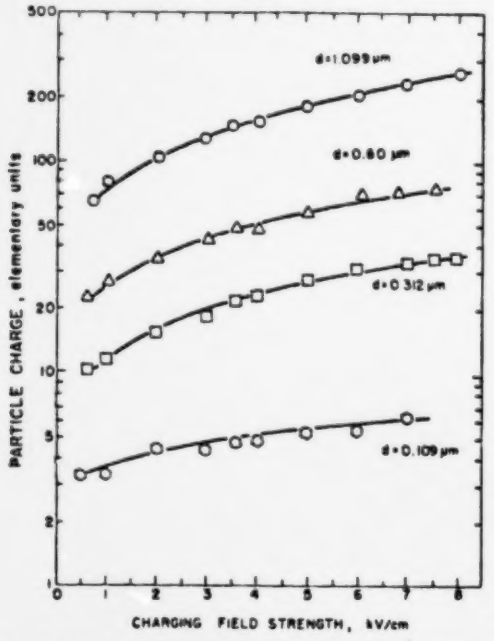

Fig. 24. Number of charges per particle for PSL and PVTL particles of various sizes. The Nt product was held constant at 5×10^{12} sec/m^3 as the charging field was varied.

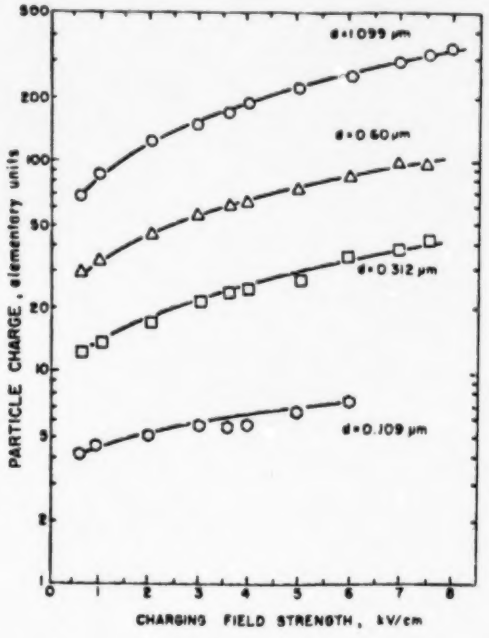

Fig. 25. Number of charges per particle for PSL and PVTL particles of various sizes. The Nt product was held constant at 1.0×10^{13} sec/m^3 as the charging field was varied.

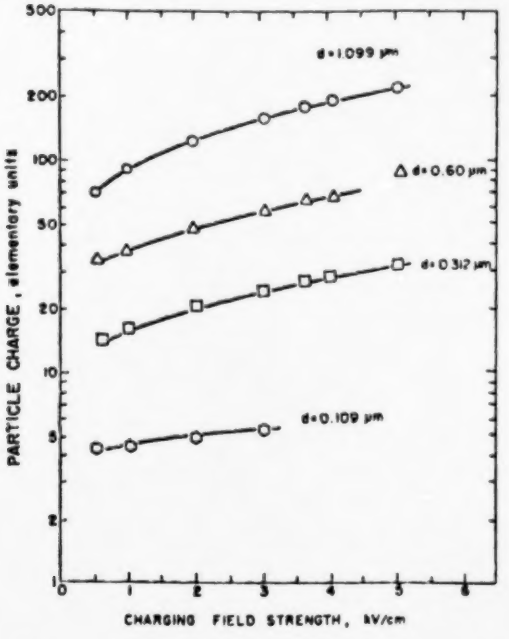

Fig. 26. Number of charges per particle vs the charging field strength for PSL and PVTL particles, with $Nt = 1.5 \times 10^{13}$ sec/m^3.

of the charge upon electric field strength is again much greater for larger particles where field charging is the dominant mechanism for charge accumulation.

3.3 *Particle charge vs dia.*

All theories of particle charging predict a strong dependence on particle dia. Some of the data taken with DOP particles are shown plotted in Fig. 27, as particle charge vs dia. for three values of the electric field strength and for Nt fixed at 1×10^{13} sec/m^3. Hewitt's data are also shown on this graph for comparison and completeness.

3.4 *Particle charging vs ion density-time product,* Nt

Hewitt verified experimentally that the accumulated charge was related to the product of the ion density (N) and charging time (t). This concept was also observed in our work where N and t were each changed by as much as a factor of two with the product Nt held constant. In each instance the resulting charge was unchanged. In view of the unique relationship between Nt and the particle charge, we have followed the convention of plotting the measured charge vs Nt.

Figures 28–32 show the charging data for the DOP aerosols, plotted as q vs Nt at several electric field strengths.

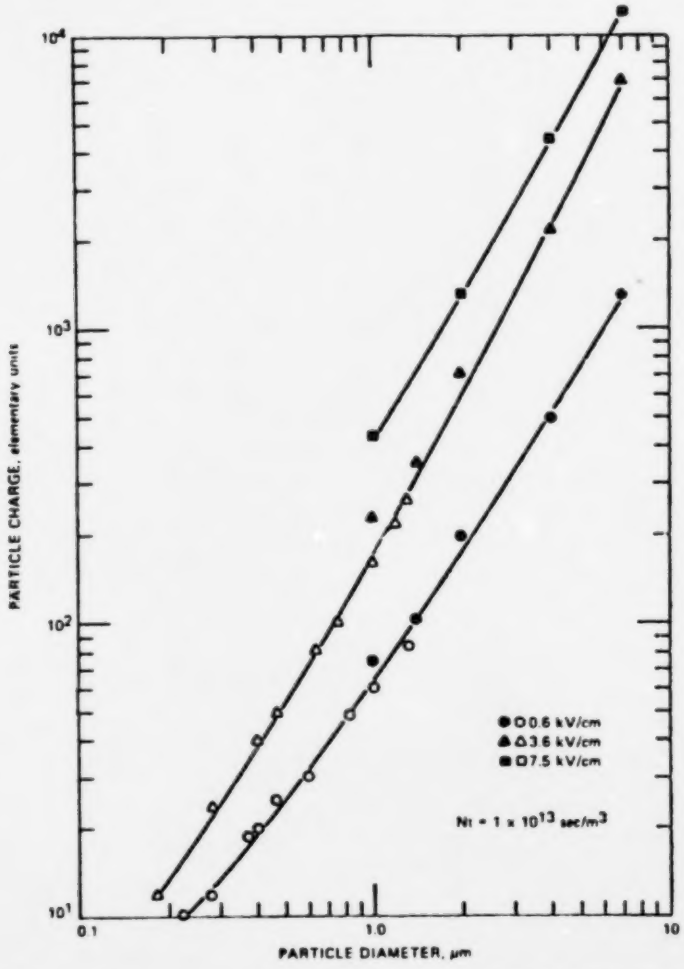

Fig. 27. Particle charge vs dia. for DOP aerosols. The open symbols are Hewitt's (1957) data.

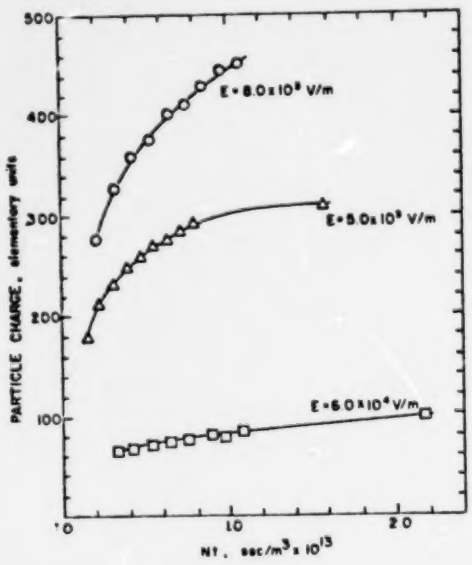

Fig. 28. Number of charges per particle vs the Nt product for a 1.0 μm dia. DOP aerosol.

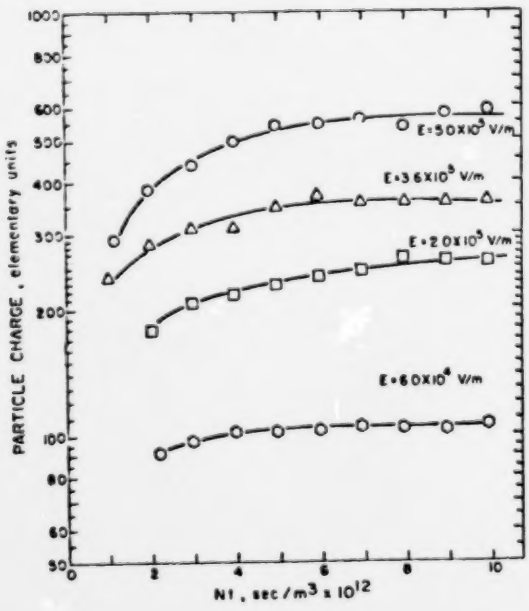

Fig. 29. Number of charges per particle vs the Nt product for a 1.4 μm dia. DOP aerosol. Four different values of the charging field strength were used.

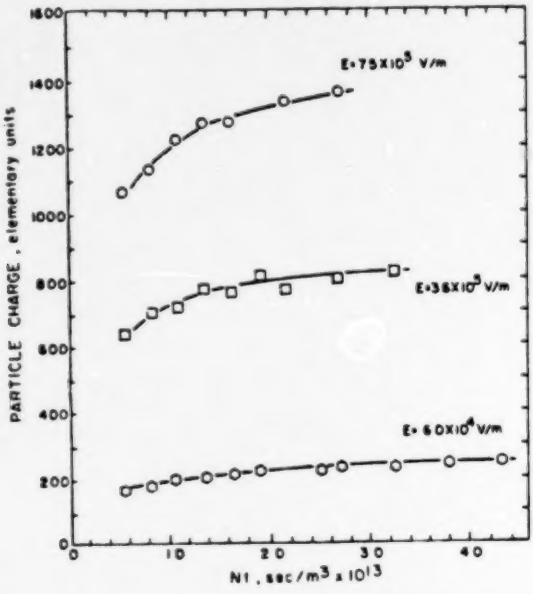

Fig. 30. Comparison of experimental and theoretical values of particle charge for a 2.0 μm dia DOP aerosol.

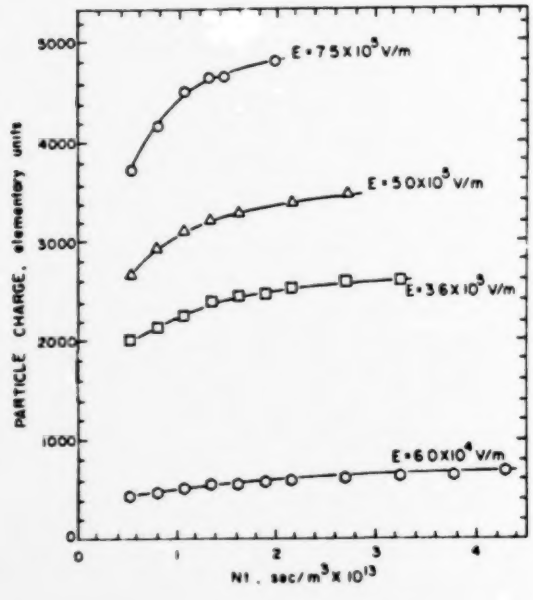

Fig. 31. Number of charges per particle vs the Nt product for 4.0 μm dia DOP particles.

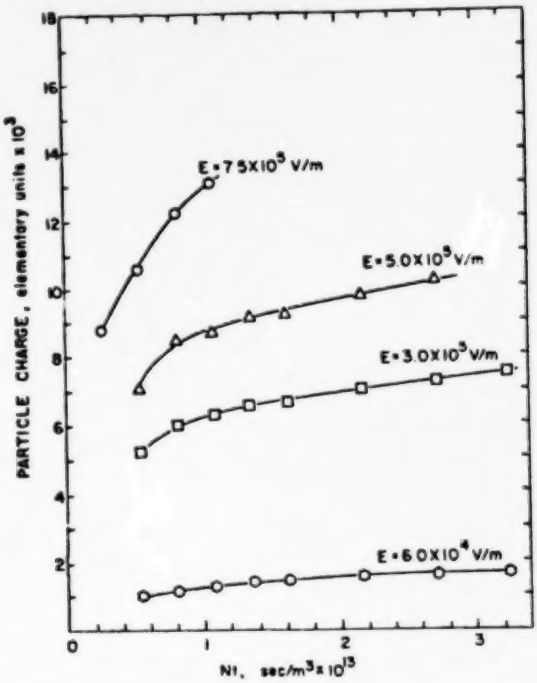

Fig. 32. Number of charges per particle vs the Nt product for a 7.0 μm dia DOP aerosol

3.5 *Particle charge vs ion mobility (positive and negative corona)*

Penney and Lynch suggested that the higher charges observed for negative corona can be explained by the presence of unattached electrons which are not present in positive corona

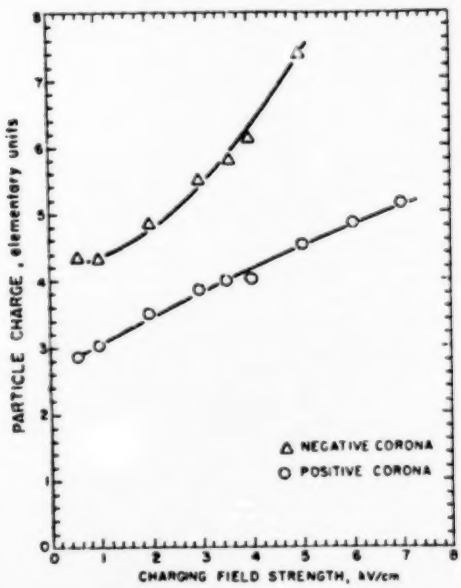

Fig. 33. Comparison of positive and negative corona charging for 0.109 μm polystyrene latex spheres. For both sets of data Nt is 5.0×10^{12} sec/m^3.

fields. In Section 3.1 it was mentioned that the average ion mobility for negative corona was measured to be significantly higher than for positive corona. Indeed, if the high current part of the $I-V$ curve is used in the curve fitting procedure to measure the ion mobility, quite high values are obtained. Figure 33 shows the results from an experiment which compares the effects of negative and positive corona for particles of 0.109 μm dia. Although the negative corona was less stable than positive and results are more erratic, the particles consistently gained significantly more charge than for positive corona charging.

Conventional theories of particle charging would predict no difference in positive and negative corona charging for these conditions. It is indicated that the charge carriers, ions and electrons, must be treated separately in applying the theory and that the assumption of single, average ion mobility and mean speed is inadequate.

3.6 *Particle charge vs dielectric constant*

The theories of particle charging predict some dependence of the charging rate upon the particle dielectric constant.

Figure 34 is a graph of particle charge vs dia. for field strengths of 3.6 and 0.6 kV/cm. Graphs are shown for DOP which has a dielectric constant of 5.1, PSL which has a dielectric constant of 2.5, and PVTL which has a dielectric constant of 2.2. Notice that there is a

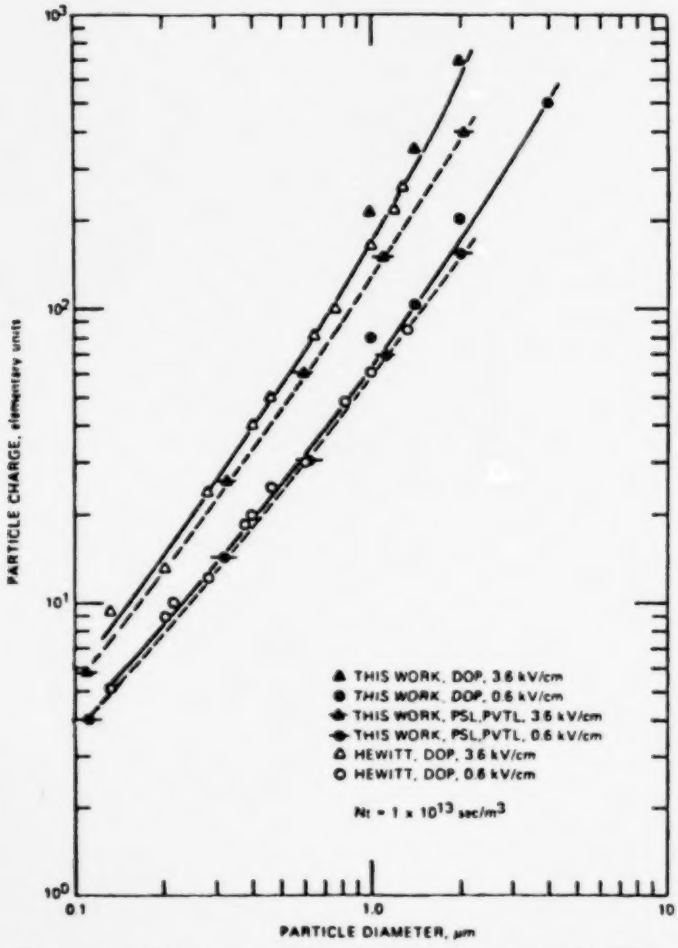
PARTICLE CHARGE, elementary units
PARTICLE DIAMETER, μm
THIS WORK, DOP, 3.6 kV/cm
THIS WORK, DOP, 0.6 kV/cm
THIS WORK, PSL,PVTL, 3.6 kV/cm
THIS WORK, PSL,PVTL, 0.6 kV/cm
HEWITT, DOP, 3.6 kV/cm
HEWITT, DOP, 0.6 kV/cm
Nt = 1 x 10^13 sec/m^3

Fig. 34 Charge vs particle dia. for aerosols of different dielectric constants. For PVTL, $K = 2.2$. For PSL, $K = 2.5$. For DOP, $K = 5.1$.

negligible difference for very small particles and for the low field case where field charging is less important. These results tend to confirm those obtained by Pauthenier and Moreau-Hanot (1932), where a similar dependence of the particle charge upon dielectric constant was observed.

4. SUMMARY AND CONCLUSIONS

Before this study was performed the majority of the experimental data which was available for comparison with particle charging theories was contained in a paper by G. Hewitt, published in 1957. Hewitt's experiments were carefully done, but the range of experimental variables was limited and his work was never independently verified.

The experiments reported here followed Hewitt's procedures closely and were designed to extend the quantity of experimental data. There is some overlap between this and Hewitt's data and, in these instances, the agreement is good.

Experimental results are presented in this paper for the charging rate of particles of 0.109–7 μm dia. at various values of electric field strength, ion density and charging time. A limited amount of data is also given which shows the important effects on the charging rate of variations in the particle dielectric constant and the polarity of the corona ion source.

Acknowledgements – This work was made possible by the financial support of the Environmental Protection Agency Research, Triangle Park, North Carolina, under Contract No. 68-02-1490.

We gratefully acknowledge the valuable advice given by H. J. White and G. W. Hewitt in the design and execution of these experiments.

REFERENCES

Arendt, P. and Kallman, H. (1935) *Z. Phys.* **35**, 836.
Berglund, R. N. and Liu, B. Y. H. (1973) *Env. Sci. and Tech.* **7**, 147.
Bricard, J., Cabane, G., Madelaine, G. and Vigla, O. (1972) *Aerosols and Atmospheric Chemistry*. (Edited by Hidy, G. M.), Academic Press, New York.
Cochet, R. (1961) Colloque International – La Physique des Forces Electrostatiques et Leurs Applications. 331.
Fuchs, N., Petrjanoff, I. and Rotzeig, B. (1936) *Trans. Faraday Soc.* 1131.
Hewitt, G. W. (1957) *A.I.E.E.* **76**, 300.
Liu, B. Y. H., Whitby, K. T. and Yu, H. H. S. (1967) *J. appl. Phys.* **38**, 1592.
Oglesby, S. and Nichols, G. B. A Manual of Electrostatic Precipitator Technology. Contract CPA 22-69-73, The National Air Pollution Control Administration (1970).
Pauthenier, M. M. and Moreau-Hanot, M. (1932) *J. Phys. Radium, Paris* **7**, 590.
Penney, G. W. and Lynch, R. P. (1957) *A.I.E.E.* **76**, 294.
Pontius, D. H., Felix, L. G., McDonald, J. R. and Smith, W. B. (1977) Final Report on EPA Contract No. 68-02-1490.
Rohmann, H. (1923) *Z. Phys.* **17**, 253.
White, H. J. (1951) *A.I.E.E.* **70**, 1186.